Shift-Symmetric Orbital Inflation: single field or multi-field?

Ana Achúcarro,[1,2,*] Edmund J. Copeland,[3,†] Oksana Iarygina,[1,‡]
Gonzalo A. Palma,[4,§] Dong-Gang Wang,[1,5,¶] and Yvette Welling[1,5,6,**]

[1] *Lorentz Institute for Theoretical Physics, Leiden University, 2333 CA Leiden, The Netherlands*
[2] *Department of Theoretical Physics, University of the Basque Country, 48080 Bilbao, Spain*
[3] *School of Physics and Astronomy, University of Nottingham, Nottingham NG7 2RD, UK*
[4] *Grupo de Cosmología y Astrofísica Teórica, Departamento de Física, FCFM, Universidad de Chile, Blanco Encalada 2008, Santiago, Chile*
[5] *Leiden Observatory, Leiden University, 2300 RA Leiden, The Netherlands*
[6] *Deutsches Elektronen-Synchrotron DESY, Notkestraße 85, 22607 Hamburg, Germany*

(Dated: January 14, 2019)

We present a class of two-field inflationary models, known as *'shift-symmetric orbital inflation'*, whose behaviour is strongly multi-field but whose predictions are remarkably close to those of single-field inflation. In these models, the field space metric and potential are such that the inflaton trajectory is along an 'angular' isometry direction whose 'radius' is constant but *arbitrary*. As a result, the radial (isocurvature) perturbations away from the trajectory are exactly *massless* and they freeze on superhorizon scales. These models are the first exact realization of the 'ultra-light isocurvature' scenario, previously described in the literature, where a combined shift symmetry emerges between the curvature and isocurvature perturbations and results in primordial perturbation spectra that are entirely consistent with current observations. Due to the turning trajectory, the radial perturbation sources the tangential (curvature) perturbation and makes it grow linearly in time. As a result, only one degree of freedom (*i.e.* the one from isocurvature modes) is responsible for the primordial observables at the end of inflation, which yields the same phenomenology as in single-field inflation. In particular, isocurvature perturbations and local non-Gaussianity are highly suppressed here, even if the inflationary dynamics is truly multi-field. We comment on the generalization to models with more than two fields.

Introduction.– The latest CMB data from the Planck collaboration [1] show that primordial perturbations are very close to Gaussian and adiabatic. The leading explanation for this observation is single field slow-roll inflation, where the perturbations are generated by a single degree of freedom. However, embedding single field inflation in an ultraviolet (UV) complete theory such as string theory is notoriously hard[1]. For instance, a plethora of moduli fields arise from string compactifications, which all have to be strongly stabilized to realize single field inflation [5]. Moreover, it is difficult to control the validity of the four dimensional effective theory when traversing large geodesic distances in field space.

One may therefore wonder whether there are multi-field inflationary scenarios that have a similar phenomenology to single field inflation. In the usual understanding, light fields during inflation lead to isocurvature perturbations or local non-Gaussianity, which are tightly constrained by current observations. However, earlier published work [6–12] already suggests that inflation with non-stabilized light fields on an axion-dilaton system can be compatible with the latest CMB data. In particular, it was pointed out in [11] that, when the perturbations orthogonal to the trajectory are *massless* but efficiently *coupled* to the inflaton perturbations, the isocurvature modes are dynamically suppressed. This is the "ultra-light isocurvature" scenario.

In this paper we provide for the first time a family of exact models of inflation in which the multi-field effects are significant, but the phenomenology remains similar to single field inflation. The models combine two ingredients: First, the inflaton trajectory proceeds along an isometry direction of the field space, so it is Orbital Inflation in the sense of [13]. This ensures time independence of the coupling between the radial and tangential inflationary perturbations. Second, the trajectory can have an *arbitrary* radius (within some range described below), and constant radius is proven to be a neutrally stable attractor. As a result, isocurvature perturbations become exactly massless. The two ingredients, combined, guarantee that the sourcing of the curvature perturbation is sustained over many e-folds of inflationary expansion. The action for the perturbations inherits a symmetry between background solutions that is not manifest in the potential or in the lagrangian. We show that, at the end of inflation, only the isocurvature degree of freedom is responsible for the generation of primordial observables, but perturbations still remain adiabatic and Gaussian. We call this scenario *shift-symmetric orbital inflation*.

[1] It is not even obvious in general how to distinguish between four-dimensional effective field theories that can be UV-completed (the "landscape") from those that cannot be (the "swampland"). This is currently the subject of intense debate and, while the details are not relevant for this paper, it highlights the importance of finding viable scenarios for inflation that are not strictly single-field. See, for instance, the discussion in [2] as compared to [3, 4]

Crucially this scenario provides a new direction in which to explore inflation and a potential resolution to some of the problems faced by the embedding of single field inflation in string theory. That is, by attempting to construct single field models of inflation where, except for the inflaton, every modulus is stabilized, one could be missing less restrictive constructions of inflation compatible with current observational constraints. We set $\hbar = c = 1$ and the reduced Planck mass $M_p \equiv (8\pi G)^{-1/2} = 1$, where G is Newton's contant. In these units the Lagrangian and all the fields are dimensionless, they are understood to be measured in units of M_p^4 and M_p, respectively.

A toy model.– To illustrate the idea, we first consider the following Lagrangian in flat field space with polar coordinates

$$\mathcal{L} = \frac{1}{2}\left[\rho^2(\partial\theta)^2 + (\partial\rho)^2\right] - \frac{1}{2}m^2\left(\theta^2 - \frac{2}{3\rho^2}\right) , \quad (1)$$

which is illustrated in Fig. 1. Notice that the potential has a monodromy in the angular coordinate. In this simple example, although the potential is unbounded from below when $\rho \to 0$, inflation only takes place in the physically consistent regime where $V(\rho, \theta)$ is positive. Moreover, as we shall show in the perturbation analysis below, our study is restricted to radii that cannot be too small. Therefore, we only care about the local form of the potential close to the inflationary trajectory, which we assume is captured well by the toy model in (1). The full potential should be well-behaved at smaller radii. In general, it is difficult to solve the background equations analytically in such a system. However, this model allows for the following exact neutrally stable solutions at any radius

$$\rho = \rho_0, \quad \dot{\theta} = \pm\sqrt{\frac{2}{3}}\frac{m}{\rho_0^2}, \quad (2)$$

which are trajectories along the θ direction as demonstrated in Fig. 1. The Friedmann equation becomes $H^2 = m^2\theta^2/6$ on the attractor, where H is the Hubble parameter, and the slow-roll parameter follows as $\epsilon \equiv -\dot{H}/H^2 = \frac{2}{\rho_0^2\theta^2}$. Moreover this isometry trajectory deviates from the geodesic in the field space, thus the turning effects become important and depend on the radius κ of the trajectory. Note that here $\kappa = \rho_0$ but, if the field space metric is curved, κ will be a more general function of ρ_0.

It is interesting to compare the above field solution with the circular orbit in a spherically symmetric gravitational field. Similarly, the radius-dependent part of the potential provides a centripetal force that stabilizes the radial direction, and the inflaton can circle at any radius with the corresponding angular velocity. For the field system on the cosmological background, only the isometric circular orbits appear, and we need to break

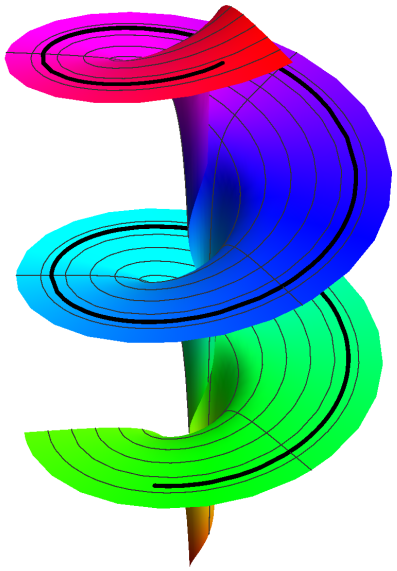

FIG. 1. The toy model potential $V(\rho, \theta)$ given in (1) together with a typical inflationary trajectory indicated with the solid black line.

the shift symmetry of θ in the potential to overcome the Hubble friction. Notice that we can label each solution by a continuous parameter c with the corresponding map

$$\rho_c = \rho_0 + c, \quad \left(\theta_c^2\right)' = \frac{\left(\theta_0^2\right)'}{(1 + c/\kappa)^2}, \quad (3)$$

where the prime $'$ denotes the derivative with respect to efolds $d/dN = d/(Hdt)$. This transformation identifies all the trajectories in (2) and it hints at the existence of a shift symmetry for the perturbations. In the flat gauge, the isocurvature perturbations σ are associated with $\delta\rho$ and the curvature perturbations $\mathcal{R}$ with $\frac{\rho}{\sqrt{2\epsilon}}\delta\theta$, which equals $\frac{1}{4}\rho^2\delta\left(\theta^2\right)$ in this toy model. In order to find the effect of the transformation on the perturbations, we split $\rho = \rho_0 + \sigma$ and $\left(\theta^2\right)' = \left(\theta_0^2\right)'(1 - \mathcal{R}')$. This allows us to determine how a small c changes σ and $\mathcal{R}'$. In the long wavelength limit every transformed set of perturbations $(\sigma_c, \mathcal{R}_c')$ should provide a new solution to the equations of motion. This is because homogeneous perturbations map background solutions onto each other. Therefore, we expect to find the following *symmetry* for linearized perturbations

$$\sigma \to \sigma + c, \quad \mathcal{R}' \to \mathcal{R}' + \frac{2}{\kappa}c. \quad (4)$$

As a consequence of the shift symmetry of σ, the isocurvature perturbations are expected to be massless and freeze after horizon-exit. Meanwhile, the symmetry also indicates that $\mathcal{R}$ has a growing solution that is dictated by the constant σ on superhorizon scales. Later we shall verify this observation of combined shift symmetry and its consequences with a full perturbation analysis.

To get an intuitive notion of the perturbation behavior, we employ the δN formalism [14–18]. From the Friedmann equation and the exact solution (2), the number of efolds until the end of inflation can be expressed as $N = \rho^2\theta^2/4 - 1/2$. Then the curvature perturbation at the end of inflation is given by

$$\mathcal{R}(k_*) = \delta N \simeq \frac{1}{\sqrt{2\epsilon_*}}(\rho\delta\theta)_* + \frac{2N_*}{\kappa}\delta\rho_*, \tag{5}$$

where $(\rho\delta\theta)_*$ and $\delta\rho_*$ are field fluctuations with typical amplitude $\frac{H_*}{2\pi}$ at horizon-exit of the k_* mode. This yields the following primordial spectrum of curvature perturbations

$$P_{\mathcal{R}}(k_*) \simeq \frac{H_*^2}{4\pi^2}\left(\frac{1}{2\epsilon_*} + \frac{4N_*^2}{\kappa^2}\right). \tag{6}$$

Here the first contribution has an adiabatic origin, just like in the single-field models, and the second term corresponds to the conversion from isocurvature to curvature modes on superhorizon scales. When the radius of the trajectory is small enough, namely $8\epsilon_* \ll \kappa^2 \ll 8\epsilon_* N_*^2 \approx 4N_*$, the second term in (6) dominates. Then the final power spectrum becomes $P_{\mathcal{R}}(k_*) \simeq H_*^2 N_*^2/(\pi^2\kappa^2)$, which is generated by one single degree of freedom – the isocurvature mode.

Shift-symmetric orbital inflation.– Let us consider how to construct generic models with the above properties. We begin with an axion-dilaton system in a non-trivial field manifold (θ, ρ) with kinetic term $K = -\frac{1}{2}\left(f(\rho)\partial_\mu\theta\partial^\mu\theta + \partial_\mu\rho\partial^\mu\rho\right)$. This field space, which has a non-trivial curvature $\mathbb{R} = f_\rho^2/2f^2 - f_{\rho\rho}/f$, arises generically from UV completion of inflation in quantum gravity or from an effective field theory viewpoint. To realize shift-symmetric orbital inflation, we assume the inflationary trajectory to be isometric , *i.e.* along the θ direction in the field space above at *any* radius. Then the potential can be derived by generalizing the Hamilton-Jacobi formalism [15, 19–21] to a two-field inflation system, as demonstrated in Appendix A. The general form of the potential can be expressed as

$$V = 3H^2 - 2\frac{H_\theta^2}{f(\rho)}, \tag{7}$$

where the Hubble parameter H is a function of θ only, $H_\theta \equiv dH/d\theta$ and $f(\rho) > 0$. The toy model (1) is recovered if we take $H \propto \theta$ and $f(\rho) = \rho^2$, which corresponds to a flat field space parametrized by polar coordinates.

Remarkably this non-linear system yields the following exact solution

$$\dot\theta = -2\frac{H_\theta}{f}, \qquad \rho = \rho_0. \tag{8}$$

Thus the inflaton indeed moves in an orbital with constant radius, as ensured by the Hamilton-Jacobi formalism. Interestingly, in these solutions the energy density of the two-field system is equal to the θ part of the potential, since the kinetic energy is precisely cancelled by the second term in (7). Also notice that this trajectory is not along a geodesic of the field space, just as in the toy model. Here the tangent and normal vector on the trajectory are expressed as $\mathcal{T}^a = 1/\sqrt{f}(1,0)$ and $\mathcal{N}^a = (0,1)$, and the radius of the turning trajectory is a constant given by $\kappa = 2f/f_\rho$. An important property is that all these trajectories are *neutrally stable*, which means that a small perturbation orthogonal to a given orbital trajectory will bring us to one of the neighbouring trajectories. This non-trivial attractor behaviour is demonstrated in Appendix B.

Analysis of perturbations.– Next, we perform a detailed study for the behaviour of perturbations. In the flat gauge, the comoving curvature perturbation $\mathcal{R}$ is defined as the projection of the field perturbation along the inflationary trajectory $\mathcal{R} = \frac{1}{\sqrt{2\epsilon}}\mathcal{T}_a\delta\phi^a$, and the isocurvature perturbation σ corresponds to the remaining orthogonal field perturbation $\sigma = \mathcal{N}_a\delta\phi^a$. Then for generic multi-field models, the quadratic action of perturbations takes the following form [11]

$$S^{(2)} = \frac{1}{2}\int d^4x a^3\left[2\epsilon\left(\dot{\mathcal{R}} - \frac{2H}{\kappa}\sigma\right)^2 + \dot\sigma^2 - \mu^2\sigma^2 + ..\right], \tag{9}$$

where ellipses denote the gradient terms $-(\partial_i\sigma)^2 - 2\epsilon(\partial_i\mathcal{R})^2$. The interaction between curvature and isocurvature modes is given by the coupling term $a^3(8\epsilon H/\kappa)\dot{\mathcal{R}}\sigma$. To guarantee perturbative analysis, we require the dimensionless coupling constant satisfies $\sqrt{8\epsilon}/\kappa \ll 1$. The effective mass of entropy perturbations is defined as $\mu^2 \equiv V_{NN} + \epsilon H^2\left(\mathbb{R} + 6/\kappa^2\right)$, where the first term is the standard Hessian of the potential $V_{NN} \equiv \mathcal{N}^a\mathcal{N}^b\left(V_{ab} - \Gamma^c_{ab}V_c\right)$, the second and third terms correspond to the field space curvature and turning contributions respectively.

For shift-symmetric orbital inflation, we expect the isocurvature perturbations to be exactly massless, as indicated from the toy model. This can be easily checked by using the exact solutions (8), and we find that the three contributions in the entropy mass μ^2 cancel each other. This implies that the quadratic action (9) has the combined shift symmetry (4), exactly as we argued from the toy model background dynamics.

The power spectra of perturbations in the massless limit can be well estimated from the coupled evolution of perturbations on superhorizon scales. When $\mu = 0$, the linearized system of coupled perturbations simplify in the superhorizon limit. It has the following solution

$$\mathcal{R}_k' = \frac{2}{\kappa}\sigma_k, \qquad \sigma_k = \frac{H_*}{2\pi}, \tag{10}$$

where the asterisk denotes evaluation at the time of horizon crossing. That is to say, on superhorizon scales the isocurvature perturbation quickly converges to a con-

stant, and it sources the growth of the curvature perturbation. At the end of inflation, the primordial curvature perturbation can be expressed as $\mathcal{R}_k = \mathcal{R}_* + 2N_*\sigma_k/\kappa$, where the first term is the curvature perturbation amplitude at horizon-exit, and the second term comes from the isocurvature source. Thus these two contributions are uncorrelated with each other, and the final dimensionless power spectrum of curvature perturbations is given by

$$P_{\mathcal{R}} = \frac{H_*^2}{8\pi^2\epsilon_*}\left(1+\mathcal{C}\right), \tag{11}$$

where $\mathcal{C} = 8\epsilon_* N_*^2/\kappa^2$ represents the contribution from isocurvature modes. This result agrees with the δN calculation for the toy model given in (6). The full calculation via the in-in formalism also gives the same answer up to subleading corrections [11]. Note that the power spectrum is completely determined by the isocurvature perturbations if $\mathcal{C} \gg 1$, which corresponds to trajectories with a small radius κ, or equivalently significant turning effects with $8\epsilon_* \ll \kappa^2 \ll 8\epsilon_* N_*^2$. Thus at the end of inflation, curvature perturbations are highly enhanced compared to the ones at horizon-exit. Meanwhile, the isocurvature power spectrum with $\mathcal{S} \equiv \sigma/\sqrt{2\epsilon}$ remains unchanged as $P_{\mathcal{S}} = \frac{H_*^2}{8\pi^2\epsilon_*}$. As a result, the amplitude of the isocurvature perturbation is dynamically suppressed, *i.e.* $P_{\mathcal{S}}/P_{\mathcal{R}} \simeq 1/\mathcal{C} \ll 1$. The details of how $P_{\mathcal{S}} \neq 0$ can generate isocurvature components in the CMB are rather model-dependent, and one cannot automatically claim that a suppressed ratio $P_{\mathcal{S}}/P_{\mathcal{R}}$ is compatible with observations. However, if $\mathcal{R}$ and $\mathcal{S}$ contributed similarly to the curvature and isocurvature components in the CMB, the result found here is found to be compatible with the current CMB constraints.

Phenomenology.– We now turn to the predictions of shift-symmetric orbital inflation for observations. First of all, let us consider the general case where $\mathcal{C}$ could take any positive value. Using the final power spectrum in (11), the tensor-to-scalar ratio can be expressed as $r = 16\epsilon_*/(1+\mathcal{C})$. And the scalar spectral index is given by $n_s - 1 \equiv \frac{d\ln P_{\mathcal{R}}}{d\ln k} = -2\epsilon_* - \eta_* + (d\mathcal{C}/dN)/(1+\mathcal{C})$, where we used $d\ln k = dN$. Note that $\frac{\partial N_*}{\partial N} = -1$, since N_* counts the number of efolds backwards. These predictions depend on the function $H(\theta)$. Like in single field inflation, this function determines how slow-roll parameters ϵ and $\eta \equiv \epsilon'/\epsilon$ scale with N_*.

For concreteness, we consider models with $H \sim \theta^p$. Using the exact solution of shift-symmetric orbital inflation (8), we integrate the equation of motion for θ and obtain the analytical expression $\theta(N)$, which yields $\epsilon_* \simeq p/(2N_*)$ and $\eta_* \simeq 1/N_*$. The predictions for n_s and r are therefore well approximated by

$$n_s - 1 \simeq -\frac{p+1}{N_*} - \frac{4p}{\kappa^2 + 4pN_*}, \quad r \simeq \frac{8p\kappa^2}{N_*\kappa^2 + 4pN_*^2}. \tag{12}$$

We plot these analytical predictions against the Planck 1σ and 2σ contours [1] in Fig. 2. Here, N_* is taken to be between 50 and 60, and the turning trajectory radius κ^2 varies between 1 and 10^5. The purple region is for $p = 1$, which corresponds to the toy model described in (1), and we also show the predictions for $p = 0.5$ (red region), $p = 0.2$ (yellow region) and $p = 0.1$ (green region).

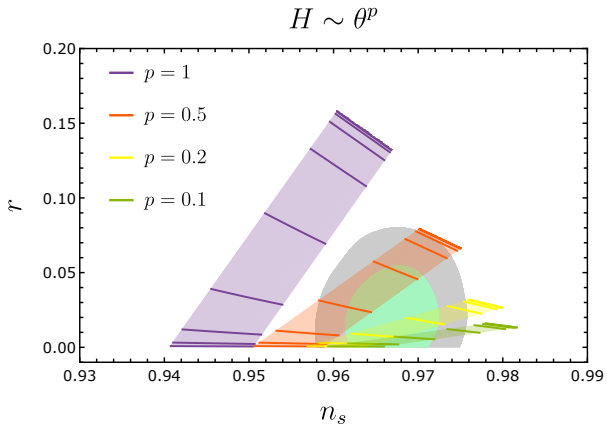

FIG. 2. The analytical predictions (12) for (n_s, r) compared to the *Planck* 1σ and 2σ contours [1]. We show the predictions for wavenumbers which cross the horizon $50-60$ efolds before the end of inflation. The predictions for $n_s - r$ depend on the value of $\kappa \in [1, 1000]$, where the values $(1, 2, 4, 8, 16, 32, 64, 128, 256)$ are depicted with thick lines (from bottom to top).

One interesting thing to notice is that our results for n_s and r only depend on the value of κ and are therefore insensitive to the details of the field metric. When $\kappa \to \infty$ one recovers the predictions of chaotic inflation with $V \propto \phi^{2p}$. Meanwhile as κ decreases, predictions are pushed downwards and to the left in this $n_s - r$ diagram. Therefore, in the case of power-law-form potentials only for small p do the predictions remain within the Planck contours. The interesting regime here is still the case with significant turning (small κ or $\mathcal{C} \gg 1$), where the final power spectrum $P_{\mathcal{R}} \simeq \frac{H_*^2 N_*^2}{\pi^2\kappa^2}$ mainly has an isocurvature origin. Then the tensor-to-scalar ratio is given by $r = 2\kappa^2/N_*^2 = 16\epsilon_*/\mathcal{C}$, which is highly suppressed. The spectral index reduces to $n_s - 1 = -(p+2)/N_*$, which lies in the sweet spot of the Planck data $n_s = 0.9649 \pm 0.0042$ if p is small.

Another important phenomenological observable is primordial non-Gaussianity. There are many examples in the literature of how $\mathcal{O}(1)$ local non-Gaussianity can arise in multi-field inflation models, especially when the coupling between isocurvature and curvature modes is large [22–24] - for a nice review with examples that include the curvaton, modulated preheating and Hybrid inflation see [25]. Considering the current bound $f_{\rm NL}^{\rm loc} = 0.8 \pm 5$ given by Planck [26], those models are marginally disfavored by observations. However, as we shall now show, this tight constraint is easily satisfied for shift-symmetric orbital inflation. The amplitude of

local non-Gaussianity is determined using the δN formalism. In a generic multi-field inflation model with curved field manifold, from the δN expansion we have $f_{\rm NL}^{\rm loc} = \frac{5}{6} G^{ab} G^{cd} N_a N_c N_{bd} / (G^{ab} N_a N_b)^2$ [22, 27], where $G_{ab} = {\rm diag}\{f(\rho), 1\}$ is the field space metric, N_a and N_{ab} are derivatives of the number of efolds with respect to the field coordinates (θ, ρ). To gain some analytical understanding, here we still focus on the $H \sim \theta^p$ models, where the number of efolds in terms of field coordinates can be expressed as $N = f(\rho)\theta^2/4p - p/2$. The amplitude of local non-Gaussianity then follows

$$f_{\rm NL}^{\rm loc} = \frac{5}{12}\eta_* \left[1 - \frac{\mathcal{C}^2}{(1+\mathcal{C})^2}\frac{\kappa^2 \mathbb{R}}{2}\right], \tag{13}$$

where we used the relation $\mathcal{C} = 2p^2/(\epsilon_* \kappa^2)$ in these $H \sim \theta^p$ models. When $\kappa \to \infty$, we have $\mathcal{C} \to 0$ and $\mathcal{C}^2 \kappa^2 \to 0$. Thus the second term in (13) vanishes, which leads to the single field result $f_{\rm NL}^{\rm loc} = 5\eta_*/12$ as expected

For the interesting regime with $\mathcal{C} \gg 1$, it is the N_ρ and $N_{\rho\rho}$ terms that dominate in the δN expansion. This then leads to what appears at first sight as the counterintuitive result, that $f_{\rm NL}^{\rm loc}$ is negligible and slow-roll suppressed

$$f_{\rm NL}^{\rm loc} \simeq \frac{5}{6}\frac{N_{\rho\rho}}{N_\rho^2} = \frac{5}{12}\eta_* \left(1 - \frac{\kappa^2 \mathbb{R}}{2}\right). \tag{14}$$

This is the same as happened in the calculation of the power spectrum: the contribution to the curvature perturbation sourced by the isocurvature modes dominates the final result. Since the bispectrum is mainly generated by one single degree of freedom, it mimics the single field prediction. But also note that there are small corrections from the field space curvature, which violates Maldacena's consistency relation [28, 29]. We will confirm this result via a scaling symmetry approach in [30]. The only possibility to have observable non-Gaussianity is in the intermediate regime with $\mathcal{C} \sim \mathcal{O}(1)$, where the transfer from isocurvature to adiabatic modes is not very efficient. In that case, $f_{\rm NL}^{\rm loc} \sim -5p\mathbb{R}/12$ can be large if the field space is highly curved.

Discussions.– In this Letter, we have proposed a class of multi-field inflationary models that demonstrate a new type of attractor trajectory along the isometry direction in field space, which is accompanied by a shift symmetry which emerges between the curvature and isocurvature perturbations. The latter modes become massless ('ultra-light') and freeze on superhorizon scales. Moreover, when the turning effects become significant, the curvature perturbations keep growing after horizon-exit and thus isocurvature modes are dynamically suppressed. As a consequence, these multi-field models yield the single-field-like phenomenology that is favored by the latest CMB observations.

Notice that the same dynamical suppression applies to the tensor-to-scalar ratio, which is lower in these models than in their single-field counterparts. Also to any additional isocurvature perturbations that are uncoupled to the curvature perturbation, since either they will decay if they are massive or, in the worst case scenario, they will freeze at a level comparable to tensor modes. Therefore, although our computations were done in a simple two-field setting, we expect the conclusions will still hold in multi-field extensions with more than two fields, provided the number of additional light isocurvature fields is not too large. We leave this case for future work.

One counterintuitive result of shift-symmetric orbital inflation is the negligible amount of local non-Gaussianity produced. Based on the δN formalism, we find that the isocurvature degree of freedom can be the dominant contribution to the bispectrum. And in such cases, $f_{\rm NL}$ is also slow-roll suppressed. This unusual result teaches us a generic lesson that in multi-field models, even if the isocurvature-to-adiabatic conversion is very efficient, the resulting non-Gaussianity can still be suppressed. The reason underlying this result is that a large coupling between the curvature and isocurvature perturbations is not enough to generate a large non-Gaussian distribution of curvature perturbations. A large coupling enhances the transfer of non-Gaussianity from the isocurvature field to the curvature perturbation, but for this transfer to generate large non-Gaussianity, one needs sizable self-interactions affecting the isocurvature field during horizon crossing [31, 32]. Therefore, it is perfectly fine to study multi-field models with significant and sustained turning trajectories, without worrying about generating large non-Gaussianity.

Another interesting question is how to distinguish shift-symmetric orbital inflation from single field slow-roll models? Although they both agree with current CMB data very well, future experiments on primordial isocurvature perturbations may allow us to discriminate between them. In shift-symmetric orbital inflation isocurvature modes can be highly suppressed but may have nonzero amplitudes, while they are totally absent in single field scenarios.

Our model has important implications on the realization of inflation in UV-complete theories. Contrary to what is usually assumed, and as was emphasized in [11], it is not always necessary to stabilize all compactification moduli, or to have a large mass hierarchy between the inflaton and other fields. The most problematic effects usually associated with multi-field effects – the generation of isocurvature perturbations and non-Gaussianity at unacceptable levels – cancel each other in the shift-symmetric orbital scenario. From an effective field theory point of view this can be traced back to the effect of derivative interactions among the curvature and isocurvature perturbations that are absent in the single-field case. These are unavoidable on curved trajectories and in curved field spaces and therefore ubiquitous in string compactifications.

Acknowledgments.– We are grateful to Valeri Vardanyan for collaboration in the early stages of this work. Also to Cristiano Germani, Gabriel Jung for stimulating discussions and comments. The work of AA is partially supported by the Netherlands' Organization for Fundamental Research in Matter (FOM), by the Basque Government (IT-979-16) and by the Spanish Ministry MINECO (FPA2015-64041-C2-1P). EJC is supported by STFC Consolidated Grant No. ST/P000703/1 and would like to acknowledge the wonderful support and hospitality of colleagues at the Lorentz Institute where some of this work was carried out. GAP acknowledges support from the Fondecyt Regular Project No. 1171811 (CONICYT). OI, DGW and YW are supported by the Netherlands Organization for Scientific Research (NWO) and OCW. YW is also supported by the ERC Consolidator Grant STRINGFLATION under the HORIZON 2020 grant agreement no. 647995.

APPENDIX A. HAMILTON-JACOBI FORMALISM

Here we apply the Hamilton-Jacobi formalism [15, 19–21] to derive the potential for shift-symmetric orbital inflation. The idea of this approach is to replace the potential as an input function with the Hubble parameter, which allows one to directly obtain all the inflation dynamics.

For the single field case, one can easily derive the Hamilton-Jacobi equation by replacing $H(t)$ with $H(\phi)$. Then the second Friedmann equation yields

$$\dot{H} = \dot{\phi} H_\phi = -\frac{\dot{\phi}^2}{2} \longrightarrow -2H_\phi = \dot{\phi}\,. \tag{15}$$

Hence the first Friedmann equation can be rewritten in the form of the Hamilton-Jacobi equation

$$V = 3H^2 - 2H_\phi^2\,, \tag{16}$$

with all functions now being explicitly dependent on ϕ. Therefore, if the Hubble parameter $H(\phi)$ is known, one can easily obtain the potential from the Hamilton-Jacobi equation.

For the multi-field case, one can use the similar trick to get the potential, but here the fundamental object is the Hubble parameter as a function of ϕ^a. Therefore the second Friedmann equation gives us

$$\dot{H} = \dot{\phi}^a H_a = -\frac{\dot{\phi}^a \dot{\phi}^b G_{ab}}{2} \longrightarrow H_a = -\frac{G_{ab}\dot{\phi}^b}{2}\,. \tag{17}$$

Then the first Friedmann equation can be rewritten as the multi-field Hamilton-Jacobi equation

$$3H^2 = V + 2H^a H_a. \tag{18}$$

Now we can use this formula to construct the generic potentials for shift-symmetric orbital inflation. The important requirement here is that the inflaton trajectory is along the isometry direction at any radius. Thus for the field space (θ, ρ) with metric $G_{ab} = \mathrm{diag}\{f(\rho), 1\}$, the inflaton should move in the θ direction for any value of ρ. For this behaviour, equation (18) simplifies to $3H^2 = V + 2\frac{H_\theta^2}{f(\rho)}$. Therefore, we conclude that our two-field inflationary model has a potential of the following form

$$V = 3H(\theta)^2 - 2\frac{H_\theta^2}{f(\rho)}. \tag{19}$$

APPENDIX B. STABILITY ANALYSIS

Here we demonstrate the neutral stability of the exact solutions. We have seen that there is a continuous set of orbital solutions parametrized by ρ_0 and that normal perturbations move us freely between these 'attractors', so the system is not stable in the usual sense. The property we need to prove is that small perturbations shift us to another inflationary solution $\dot{\rho} = 0$.

Each attractor solution (8) corresponds to a point in the $(\dot{\rho}, \dot{\theta})$ plane. These points are all different and lie on a curve, therefore the stability of this system is non-trivial to prove analytically. If we simply perturb the field equations we will find zero eigenvalues associated with the perturbations that move us between attractors. Moreover, it is not obvious how to find variables such that the linearized system of perturbations becomes diagonal. In addition, we expect the Hubble friction to play a crucial role, hence we perform the stability analysis in the number of efolds rather than in cosmic time. Therefore, we introduce the variables

$$x(\theta, \rho, \theta', \rho') \equiv \tfrac{fH}{H_\theta}\theta' - 2\tfrac{f}{f_\rho}\rho' + 2, \tag{20}$$

$$y(\theta, \rho, \theta', \rho') \equiv \tfrac{fH}{H_\theta}\theta' + 2\,, \tag{21}$$

$$z(\theta, \rho) \equiv \tfrac{fH^2}{H_\theta^2} - 2/3\,. \tag{22}$$

Here a prime denotes a derivative with respect to the number of efolds $(..)' = \frac{d}{dN}(..)$. Remember that $H = H(\theta)$ and $f = f(\rho)$. Our definition of stability now amounts to the presence of a fixed point at $(x, y) = (0, 0)$.

The definition of x and y above are based on an observation for the models where the Hubble parameter is linear in θ. For $H \sim \theta$ the potential in (19) satisfies the following scaling relation

$$\theta V_\theta - 2\frac{f}{f_\rho} V_\rho = 2V. \tag{23}$$

This ensures that the equations for x and y diagonalize at the linear level. This we can use to prove linear stability for the models $H \sim \theta$, which we show below. In fact

it turns out to apply to any power law $H \sim \theta^n$. Moreover, we argue that neutral stability also applies to more general models.

Linear stability analysis

The first step is to rewrite the field equations and second Friedmann equation in terms of the x, y, ρ and z variables. The equations of motion read

$$x' + (3-\epsilon)x + \left(2\left(\frac{f}{f_\rho}\right)_\rho - g(\theta)\right)(\rho')^2 + \tfrac{2(z+2/3)}{z} g(\theta)(\epsilon - \epsilon_0) = 0, \tag{24}$$

$$y' + (3-\epsilon)y + \tfrac{2}{z}\left(-\tfrac{1}{3}(\rho')^2 - \tfrac{1}{2}y^2 + 2y\right) - g(\theta)(\rho')^2 + \tfrac{2(z+2/3)}{z} g(\theta)(\epsilon - \epsilon_0) = 0, \tag{25}$$

$$z' = 2(y-2)(1-g(\theta)) + \left(\frac{f_\rho}{f}\right)^2 \tfrac{y-x}{2}\left(z + \tfrac{2}{3}\right), \tag{26}$$

$$\rho' = \tfrac{f_\rho}{f}\tfrac{y-x}{2}, \tag{27}$$

$$\epsilon = \tfrac{1}{2}\tfrac{(y-2)^2}{z+2/3} + \tfrac{f_\rho^2}{f^2}\tfrac{(x-y)^2}{8}, \tag{28}$$

where $\epsilon_0 = \frac{2}{z+2/3}$. All the terms in brackets are combined to be manifestly zero on the attractor, and we have introduced the model specific function $g(\theta) \equiv \frac{H H_{\theta\theta}}{H_\theta^2}$. Note that $g(\theta)$ is in general a function of z and ρ, but it reduces to a constant in the case when we have a power law $H(\theta) \sim \theta^n$, and it is zero for $n = 1$.

In terms of the four variables, shift-symmetric Orbital Inflation is given by $(x, y, z', \rho') = (0, 0, -4(1-g(\theta)), 0)$, and we would like to prove that this is the attractor solution. It will be sufficient to show that $(y, \rho') = (0, 0)$ is a fixed point. Note that the friction term is very large during inflation. We can already see that without the friction the system would be unstable, so we now establish whether the friction term is in fact large enough to make the system stable.

To study the stability of the point $(y, \rho') = (0, 0)$, we linearly perturb the equations around the desired attractor with $\epsilon = \frac{2}{z+2/3}$. We obtain

$$\delta x' + \left(3 - \tfrac{2}{z+2/3}\right)\delta x - \tfrac{4g(\theta)}{z}\delta y = 0, \tag{29}$$

$$\delta y' + \left(3 - \tfrac{2}{z+2/3} + \tfrac{4(1-g(\theta))}{z}\right)\delta y = 0, \tag{30}$$

$$\delta z' = 2(1-g(\theta))\delta y + \left(\frac{f_\rho}{f}\right)^2 \tfrac{\delta y - \delta x}{2}\left(z + \tfrac{2}{3}\right), \tag{31}$$

$$\delta\rho' = \tfrac{f_\rho}{f}\tfrac{\delta y - \delta x}{2}. \tag{32}$$

Surprisingly, the linearized system of perturbations is very simple for any $g(\theta)$. In particular, for constant $g(\theta)$ we can explicitly prove stability, as we do below. For a more general function we have to express $g(\theta)$ in terms of z and ρ and integrate the equations numerically. However, we expect the system to be stable. If $(1-g(\theta))$ takes values of order 1 and does not vary too rapidly, then z will take large values during inflation and behave smoothly as well. In that case we see from (29) and (30) that $\delta x'$ and $\delta y'$ are dominated by the friction terms $-3\delta x$ and $-3\delta y$ respectively. Therefore, we expect both of them to decay like e^{-3N}. Finally (32) then implies that we quickly converge to the fixed point.

Power law inflation $H \sim \theta^n$

In the case of power law inflation with $1 - g(\theta) = \frac{1}{n}$ we can integrate the δy equation (30), using $z = z_0 - \frac{4}{n}N$. This we can then use to solve for δx as well. We find the following solution

$$\delta x = \delta x_0 \left(\tfrac{2+3z_0}{2+3z}\right)^{n/2} e^{-3N} + \delta y_0 \tfrac{4(n-1)N}{n}\left(\tfrac{2+3z_0}{2+3z}\right)^{n/2} e^{-3N},$$
$$\delta y = \delta y_0 \tfrac{z}{z_0}\left(\tfrac{2+3z_0}{2+3z}\right)^{n/2} e^{-3N}. \tag{33}$$

Plugging these solutions back into (32) we conclude that $(y, \rho') = (0, 0)$ is a fixed point. This proves stability for power law inflation.

Linearized equations in the slow-roll parameters

We can write the linearized perturbation equations in terms of the slow-roll parameters ϵ and η

$$\epsilon = \frac{2H_\theta^2}{fH^2}, \quad \eta \equiv \frac{\dot\epsilon}{H\epsilon} = -\frac{4H_{\theta\theta}}{fH} + \frac{4}{f}\left(\frac{H_\theta}{H}\right)^2. \tag{34}$$

In particular, the model specific function $g(\theta)$ becomes

$$g(\theta) = (2\epsilon - \eta)\sqrt{\frac{f}{8\epsilon}}\,. \tag{35}$$

We see that $g(\theta)$ is not necessarily positive, but it will be small if both the slow-roll approximation and the condition $\eta \ll \sqrt{\epsilon}$ hold true. The linearized equations (29) – (32) are then given by

$$\delta x' + (3-\epsilon)\,\delta x - \tfrac{2\epsilon-\eta}{1-\epsilon/3}\sqrt{\tfrac{\epsilon f}{2}}\delta y = 0, \tag{36}$$

$$\delta y' + \left(3 - \epsilon + \tfrac{1}{1-\epsilon/3}\left(2\epsilon - (2\epsilon-\eta)\sqrt{\tfrac{\epsilon f}{2}}\right)\right)\delta y = 0,$$

$$\delta z' = 2\left(1 - (2\epsilon-\eta)\sqrt{\tfrac{f}{8\epsilon}}\right)\delta y + \left(\tfrac{f_\rho}{f}\right)^2 \tfrac{\delta y - \delta x}{\epsilon},$$

$$\delta\rho' = \tfrac{f_\rho}{f}\tfrac{\delta y - \delta x}{2}.$$

In the slow-roll approximation δx and δy are therefore exponentially decaying

$$\delta x \approx \delta x_0 e^{-3N}, \tag{37}$$

$$\delta y \approx \delta y_0 e^{-3N}. \tag{38}$$

Looking at the equation for δz we find that a sufficient condition for stability is that e^{-3N}/ϵ goes to zero exponentially fast. This requires $\eta < 3$, which is automatically satisfied assuming the slow-roll approximation $\eta \ll 1$. In addition, ϵ cannot be arbitrarily small.

* achucar@lorentz.leidenuniv.nl
† ed.copeland@nottingham.ac.uk
‡ iarygina@lorentz.leidenuniv.nl
§ gpalmaquilod@ing.uchile.cl
¶ wdgang@strw.leidenuniv.nl
** welling@strw.leidenuniv.nl

[1] Y. Akrami *et al.* (Planck), (2018), arXiv:1807.06211 [astro-ph.CO].
[2] A. Achúcarro and G. A. Palma, (2018), arXiv:1807.04390 [hep-th].
[3] G. Obied, H. Ooguri, L. Spodyneiko, and C. Vafa, (2018), arXiv:1806.08362 [hep-th].
[4] P. Agrawal, G. Obied, P. J. Steinhardt, and C. Vafa, Phys. Lett. **B784**, 271 (2018), arXiv:1806.09718 [hep-th].
[5] D. Baumann and L. McAllister, *Inflation and String Theory*, Cambridge Monographs on Mathematical Physics (Cambridge University Press, 2015) arXiv:1404.2601 [hep-th].
[6] T. Kobayashi and S. Mukohyama, Phys. Rev. **D81**, 103504 (2010), arXiv:1003.0076 [astro-ph.CO].
[7] S. Renaux-Petel and K. Turzynski, JCAP **1506**, 010 (2015), arXiv:1405.6195 [astro-ph.CO].
[8] S. Cremonini, Z. Lalak, and K. Turzynski, Phys. Rev. **D82**, 047301 (2010), arXiv:1005.4347 [hep-th].
[9] S. Cremonini, Z. Lalak, and K. Turzynski, JCAP **1103**, 016 (2011), arXiv:1010.3021 [hep-th].
[10] C. van de Bruck and M. Robinson, JCAP **1408**, 024 (2014), arXiv:1404.7806 [astro-ph.CO].
[11] A. Achúcarro, V. Atal, C. Germani, and G. A. Palma, JCAP **1702**, 013 (2017), arXiv:1607.08609 [astro-ph.CO].
[12] A. Achúcarro, R. Kallosh, A. Linde, D.-G. Wang, and Y. Welling, JCAP **1804**, 028 (2018), arXiv:1711.09478 [hep-th].
[13] A. Achúcarro and Y. Welling, (In Preparation).
[14] A. A. Starobinsky, JETP Lett. **42**, 152 (1985), [Pisma Zh. Eksp. Teor. Fiz.42,124(1985)].
[15] D. S. Salopek and J. R. Bond, Phys. Rev. **D42**, 3936 (1990).
[16] M. Sasaki and E. D. Stewart, Prog. Theor. Phys. **95**, 71 (1996), arXiv:astro-ph/9507001 [astro-ph].
[17] M. Sasaki and T. Tanaka, Prog. Theor. Phys. **99**, 763 (1998), arXiv:gr-qc/9801017 [gr-qc].
[18] H.-C. Lee, M. Sasaki, E. D. Stewart, T. Tanaka, and S. Yokoyama, JCAP **0510**, 004 (2005), arXiv:astro-ph/0506262 [astro-ph].
[19] A. G. Muslimov, Class. Quant. Grav. **7**, 231 (1990).
[20] J. E. Lidsey, Phys. Lett. **B273**, 42 (1991).
[21] E. J. Copeland, E. W. Kolb, A. R. Liddle, and J. E. Lidsey, Phys. Rev. **D48**, 2529 (1993), arXiv:hep-ph/9303288 [hep-ph].
[22] D. H. Lyth and Y. Rodriguez, Phys. Rev. Lett. **95**, 121302 (2005), arXiv:astro-ph/0504045 [astro-ph].
[23] C. T. Byrnes, K.-Y. Choi, and L. M. H. Hall, JCAP **0810**, 008 (2008), arXiv:0807.1101 [astro-ph].
[24] C. T. Byrnes and G. Tasinato, JCAP **0908**, 016 (2009), arXiv:0906.0767 [astro-ph.CO].
[25] C. T. Byrnes and K.-Y. Choi, Adv. Astron. **2010**, 724525 (2010), arXiv:1002.3110 [astro-ph.CO].
[26] P. A. R. Ade *et al.* (Planck), Astron. Astrophys. **594**, A17 (2016), arXiv:1502.01592 [astro-ph.CO].
[27] D. Seery and J. E. Lidsey, JCAP **0509**, 011 (2005), arXiv:astro-ph/0506056 [astro-ph].
[28] J. M. Maldacena, JHEP **05**, 013 (2003), arXiv:astro-ph/0210603 [astro-ph].
[29] P. Creminelli and M. Zaldarriaga, JCAP **0410**, 006 (2004), arXiv:astro-ph/0407059 [astro-ph].
[30] A. Achúcarro, , G. A. Palma, D.-G. Wang, and Y. Welling, (In Preparation).
[31] X. Chen and Y. Wang, JCAP **1004**, 027 (2010), arXiv:0911.3380 [hep-th].
[32] X. Chen, G. A. Palma, W. Riquelme, B. Scheihing Hitschfeld, and S. Sypsas, Phys. Rev. **D98**, 083528 (2018), arXiv:1804.07315 [hep-th].